**Orthophoto mosaic, elevation mosaic, and hazard analysis package for a potential Lacus Mortis landing site produced as part of Moon Trek.** A. G. Curtis[1] and N. Gallegos[2], NASA Solar System Treks Team[3], B. H. Day[4], [1] JPL (aaron.curtis@jpl.nasa.gov), [2]JPL (natalie.gallegos@jpl.nasa.gov), [3]JPL (emily.s.law@jpl.nasa.gov), [4]NASA Solar System Exploration Research Virtual Institute. (NASA Ames Research Center. M/S 17-1. Moffett Field, CA, USA. 94035. Brian.H.Day@nasa.gov)

**Introduction:** Solar System Treks, at https://trek.nasa.gov, serve a broad range of data types for the planetary science community. Interest in a potential landing site in Lacus Mortis near 25.2E 43.8N spurred an effort to create a package of data to be added to Moon Trek for planning, situational awareness and hazard analysis. Using Lunar Reconaissance Orbiter Narrow Angle Camera (LRO NAC) images, we produced an elevation mosaic with a North-South extent of 283 km, an East-West extent of 164 km, and a pixel resolution of better than 6m in the East-West direction and 8m in the North-South direction. We also created an orthoimage mosaic using one image from each of the stereo pairs. For two of the NAC images used in the mosaic, we detected craters using a neural network approach, and rocks using a heuristic algorithm.

**Digital elevation model (DEM) mosaic:** Using an in-house stereo workflow, we reconstructed, aligned, and merged seven individual LRO NAC DEMs. Our stereo pipeline begins with pair selection using a python script which queries Trek's DSBservice API, uses geopandas to compute overlap regions, and culls the pairs based on overlap area, sun angle, and spacecraft geometry as recommended by [1]. Our pair selection script additionally contains a new grid search algorithm which selects a set of pairs which fully cover the requested bounding box approximately once.

Our workflow uses USGS ISIS for data ingestion, and Ames Stereo Pipeline (ASP) [2] for stereo reconstruction. Before reconstruction, we used cam2map4stereo.py to project each pair to the lowest common resolution. Following dense reconstruction, we aligned each point cloud individually to LRO LOLA laser altimetry data using ASP's pc_align utility. Parameters for pc_align were manually tuned. The aligned point clouds were converted to DEMs using ASP point2dem, and merged using dem_mosaic. To eliminate outlier points, which were especially prevalent at the edges of stereo point clouds, we employed point2dem's median filter.

To check for distortion across the DEM mosaic, we computed the elevation difference between each LOLA shot in the area and the corresponding elevations in our DEM mosaic (Fig. 1). All points sampled were within 25m in elevation of LOLA, with the vast majority within 10m.

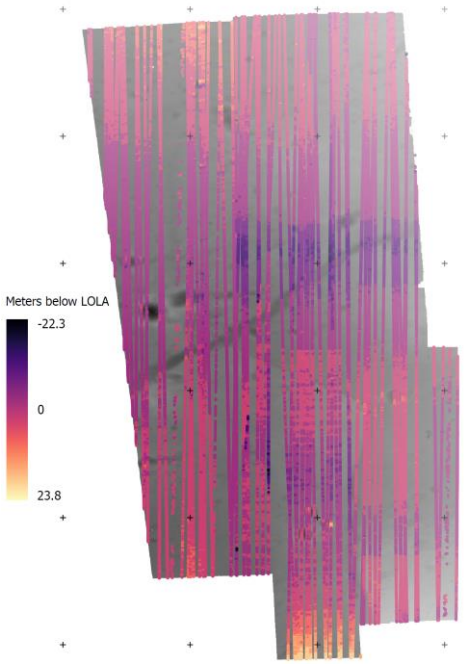


***Fig. 1.*** *DEM mosaic of Lacus Mortis site with LOLA shot elevation differences overlain*

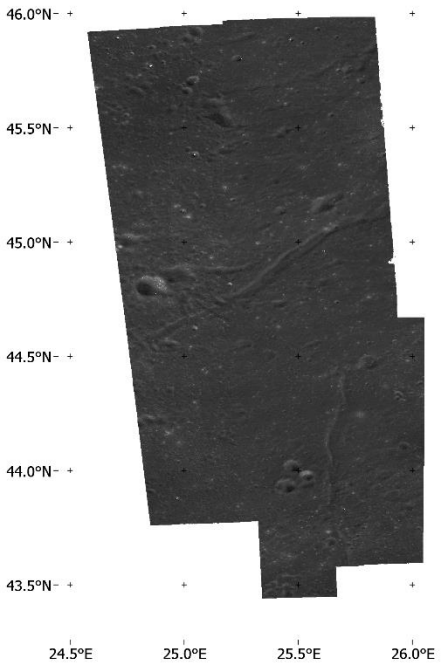


***Fig. 2.*** *Orthophoto mosaic of the Lacus Mortis target site*

**Orthophoto mosaic:** For ease of use in conjunction with the DEM mosaic, we produced an orthophoto mosaic combining the "left" image of each stereo pair, projected onto the point cloud data for that pair (Fig. 2). Individual orthoimages were created using the --orthophoto option to ASP point2dem. The images were color balanced and combined using Orfeo Toolbox's Mosaic tool [3].

**Rock detection:** The rock detection tool uses a pure image approach to detect possible rocks on the lunar or Martian surface using LROC NAC images or HiRISE EDR strips. It takes in an image name and a number of parameter inputs that control the quality and quantity of rock detections. The parameters are exposed to the user through the UI and three preconfigured settings are offered. The detector uses image metadata and does some optional preprocessing (sharpening, brightening, blurring, and various contrast options).

After some preprocessing, detection takes place. The image gradient is computed leveraging numpy's gradient techniques in combination with the image's solar azimuth angle. Thresholding is applied to the image, and regions that are most likely to be classified as rocks are found by running connected component analysis over the binary image. Post processing further filters the rock candidates by looking at bounding box eccentricity, area, and ratio. The rock detector returns the image it processed, the processed image with bounding boxes around rock detections (Fig. 3), a text file of rock descriptors (locations on the image), and rock density chart for the image.

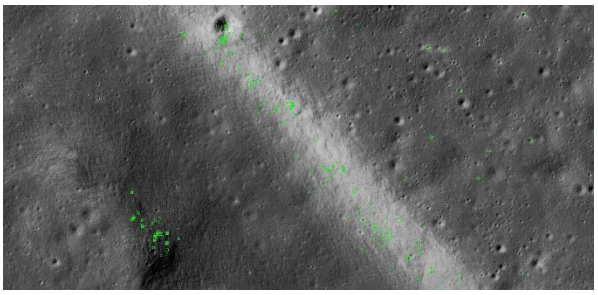

***Fig. 3.*** *Detail from rock detection results using image gradient approach*

**Crater detection:** The crater detector (Fig. 4) finds possible craters on individual LROC NACs or HiRISE swaths. The tool can be broken up into two main processes: detection and recognition. Detection is a purely image-based approach. Detection techniques are used to find as many crater candidates as possible. These techniques include edge detection (searching for sharp crater rims) , crater shadow and highlight pairing through image thresholding [4], and template matching [5]. Some of these techniques use metadata about the image taken from PDS labels, such as solar incidence and azimuth angles. This data is used to filter candidates based on illumination. Once detection is complete, crater candidates are fed into a convolutional neural network for the recognition phase.

The convolutional neural network is trained on approximately 10,000 craters pulled from a single NAC image. This includes image augmentation. The output is a confidence value for each input image ranging from 0 - 1, where 1 means that model is very confident that this is a crater, and 0 denotes the lowest confidence that the candidate is a crater. The software only returns and prints data for crater candidates that have a confidence value greater than or equal to 0.5. Once detection and recognition are complete, three files are returned. A heatmap based on crater density, an image with craters labeled (bounding boxes over detected craters), and a text file with crater details (latitude, longitude, estimated diameter and depth, confidence value).

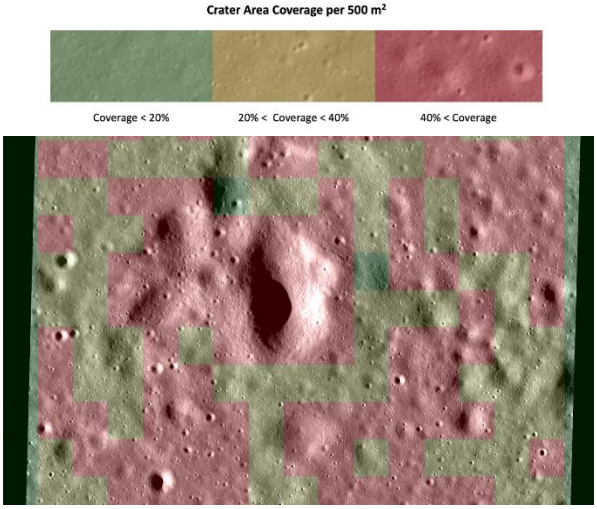


***Fig. 4.*** *Detail from crater detection results*

**References** [1] Becker, K. J. et al. *Earth and Space Sci.*, 46 2703 (2015). [2] Beyer, R. A., Alexandrov, O. & McMichael, S. *Earth and Space Sci* 5, 537–548 (2018). [3] Grizonnet, M. et al. *Open Geospatial Data, Software and Standards* 2, 15 (2017). [4] Kamarudin, N. D., Makhtar, S. N. & Hidzir, H. D. M. *Proc. IEEE IconSpace* 190–195 (2011). [5] Urbach, E. R. & Stepinski, T. F. *Planetary and Space Science* 57, 880–887 (2009).

**Acknowledgements**: The authors would like to thank the Planetary Science Division of NASA's Science Mission Directorate, NASA's SMD Science Engagement and Partnerships, the Advanced Explorations Systems Program of NASA's Human Exploration Operations Directorate, and the Moons to Mars Mission Directorate for their support and guidance in the development of the Solar System Treks.